CrossMark

PET imaging of tau protein targets: a methodology perspective

Cristina Lois[1] · Ivan Gonzalez[2] · Keith A. Johnson[1] · Julie C. Price[2]

Abstract

The two neuropathological hallmarks of Alzheimer's disease (AD) are amyloid-β plaques and neurofibrillary tangles of tau protein. Fifteen years ago, Positron Emission Tomography (PET) with Pittsburgh Compound B (^{11}C-PiB) enabled selective in-vivo visualization of amyloid-β plaque deposits and has since provided valuable information about the role of amyloid-β deposition in AD. The progression of tau deposition has been shown to be highly associated with neuronal loss, neurodegeneration, and cognitive decline. Until recently it was not possible to visualize tau deposition in-vivo, but several tau PET tracers are now available in different stages of clinical development. To date, no tau tracer has been approved by the Food and Drug Administration for use in the evaluation of AD or other tauopathies, despite very active research efforts. In this paper we review the recent developments in tau PET imaging with a focus on in-vivo findings in AD and discuss the challenges associated with tau tracer development, the status of development and validation of different tau tracers, and the clinical information these provide.

Keywords Tau Imaging · PET · Radiotracers · Alzheimer's disease · Aging

Introduction

Alzheimer's disease (AD) affected an estimated 5.4 million Americans in 2016 (Alzheimer's Association 2016) and, due to increased lifespan, may affect 13.5 million by 2050 (Alzheimer's Association 2015). The two hallmark pathologies of AD are the progressive accumulation of amyloid-β plaques and the abnormal aggregation of tau protein into paired helical filaments and neurofibrillary tangles. These deposits are eventually accompanied by neuroinflammation, neuronal/neuritic dysfunction, and cellular death (Heneka et al. 2015).

The initial cause of late-onset sporadic AD is still unknown. One long-standing hypothesis has driven many efforts in the search for disease-modifying therapies. The 'amyloid-cascade hypothesis' proposes that AD is primarily driven by amyloid-β and the disease process, including tau deposition, is the result of an imbalance between the production and clearance of amyloid-β (Hardy 2002). Support for this hypothesis includes: (1) inherited mutations in APP and presenilin (the precursor protein and the protease for amyloid-β generation, respectively) yield early-onset amyloid-β deposition and AD (Goate et al. 1991); (2) Down's syndrome individuals have an extra copy of chromosome 21, which codes for APP, and present elevated amyloid-β deposition and risk of AD (Olson and Shaw 1969); (3) an APP gene mutation was recently reported to protect against AD and cognitive decline in elders (Jonsson et al. 2012). It is also known that amyloid-β deposition can lead to progressive tau deposition, but the converse has not been demonstrated in humans (Selkoe and Hardy 2016). However, the amyloid hypothesis is still controversial and is challenged by data showing inconsistencies with the proposed linear structure (Herrup 2015; Fessel 2018) and the failure of phase III trials of anti-amyloid-β therapies (Drachman 2014; Harrison and Owen 2016).

Postmortem studies indicate that both amyloid-β plaques and tau accumulate following distinct stereotypic spatial and temporal patterns. Amyloid-β accumulation is mainly in the neocortex and begins as early as 30 years before symptoms occur. In contrast, tau accumulation begins much earlier

✉ Cristina Lois
  cloisgomez@mgh.harvard.edu

1 Gordon Center for Medical Imaging, Division of Nuclear Medicine and Molecular Imaging, Department of Radiology, Massachusetts General Hospital / Harvard Medical School, Boston, MA, USA

2 Athinoula A. Martinos Center for Biomedical Research, Department of Radiology, Massachusetts General Hospital / Harvard Medical School, Boston, MA, USA

in deep gray matter structures, prominently in brainstem, entorhinal cortex, medial temporal lobe, and increases gradually with age (Braak el al. 2011). In AD, PET imaging indicates that tau spreads dramatically across the neocortex, apparently accelerated by amyloid-β burden (Hanseeuw et al. 2017; Sperling et al. 2014; Yanai et al. 2016; Okamura and Yanai 2017). The progression of AD is described at autopsy using a staging system of the progression of tau neurofibrillary tangles, threads and dystrophic neurites (Braak and Braak 1991, 1999). A number of studies have explored quantification of tau PET and have allowed comparison to and recapitulation of key features of the autopsy staging framework (e.g., Johnson et al. 2016; Schwarz et al. 2016; Scholl et al. 2016; Cho et al. 2016).

The development of ^{11}C-Pittsburgh Compound B (^{11}C-PiB) enabled the selective in-vivo visualization and quantification of amyloid-β deposits (Klunk et al. 2004; Mathis et al. 2005; Price et al. 2005; Lopresti et al. 2005). The subsequent development of selective ^{18}F-labeled amyloid-imaging agents, with a fivefold longer half-life, facilitated distribution and widespread use of amyloid-β PET. These developments profoundly impacted the understanding of the spatial and temporal evolution of amyloid-β pathology. For example, amyloid-β deposits are found in-vivo in 25–40% of elders with normal cognition and associated with cognitive decline over the following 3–5 years (Mintun et al. 2006; Donohue et al. 2017). This suggests amyloid-β may be an early and necessary, but not sufficient, cause for cognitive decline in AD, pointing to other downstream mechanisms such as tau deposition (Villemagne et al. 2012).

Tau deposition is highly associated with neuronal loss, neurodegeneration, and cognitive decline (Braak and Braak 1991; Delacourte et al. 1999; Arriagada et al. 1992; Bierer et al. 1995; Hyman et al. 2012; Johnson et al. 2016; Ossenkoppele et al. 2016) which, together with the recent failure of anti-amyloid drug trials (Expedition 3), has fueled the interest in tau as a therapeutic target (Giacobini and Gold 2013). Selective tau PET tracers have been developed in recent years, enabling in-vivo visualization of tau deposition. Tau tracers are in different stages of clinical development (Wood 2013; Okamura et al. 2013, 2014; Villemagne et al. 2014; Jovalekic et al. 2016; Harada et al. 2016), as recently reviewed by Saint-Aubert et al. (2017), although none has yet been FDA-approved for clinical use in the evaluation of AD or other tauopathies. Tau PET imaging has the potential to facilitate accurate tauopathy diagnosis, precise assessment of disease severity, disease progression, efficacy of potential disease-modifying anti-tau treatments, and inform patient enrollment for trials (Harada et al. 2016). Thus, PET imaging now enables tracking of both tau and amyloid-β deposition over time, offering a unique opportunity to elucidate how the relationship between these misfolded proteins impacts the development of cognitive decline.

This paper provides an overview of tau PET imaging from a PET methodology perspective. This includes discussion of important in-vivo observations in AD, tracer validation efforts, limitations and challenges of early tau tracers, and remaining methodological considerations.

Rapid emergence of tau PET imaging and progress

Tau PET imaging is rapidly evolving, as illustrated by the burst in publications in this topic in 2016, which doubled the total number in the preceding years (Saint-Aubert et al. 2017).

Challenges of in-vivo tau imaging

An ideal tau tracer must fulfill the general requirements for any brain PET tracer, including ample blood–brain barrier penetration, low toxicity, low non-specific binding, rapid uptake and clearance from the brain, and no radiolabeled metabolites in the brain. Furthermore, the use of ^{18}F instead of ^{11}C is preferred due to the longer half-life (Villemagne et al. 2012; Dani et al. 2016).

Tau imaging presents additional challenges. As recently summarized (Harada et al. 2016), tau proteins present different isoform composition, different ultrastructure (paired helical or straight filaments), and different patterns of deposition in various taoupathies. There are six isoforms of tau protein that are produced by alternative splicing of the tau MAPT gene. These isoforms are categorized into two functionally different groups based on the number of microtubule-binding domains transcribed in the tau protein: 3 repeats (3R) or 4 repeats (4R). Normal adult brains contain approximately equal ratio of 3R and 4R tau isoforms, while abnormal tau deposits in various tauopathies contain different isoform compositions: both 3R and 4R tau is present in AD, tangle predominant senile dementia, and chronic traumatic encephalopathy; 3R tau is dominant in Pick's disease, and 4R tau is dominant in corticobasal degeneration, progressive supranuclear palsy (PSP) and argyrophilic grain disease (Liu et al. 2008). Due to these differences, a single tau PET tracer may not bind to all these heterogeneous tau deposits, or may bind them with different affinities. Additionally, tau is largely an intracellular protein, so the tau tracer must cross the cell membrane, as well as the blood–brain barrier, which confers requirements about its molecular size and lipophilicity. Also, since current tau PET tracers share β-sheet binding properties, they need to achieve selectivity for tau aggregates over amyloid-β and other misfolded proteins with similar structural motifs. This is particularly critical in AD, as tau deposits are co-localized

with amyloid-β plaques but at much lower concentrations (Villemagne et al. 2012; Dani et al. 2016).
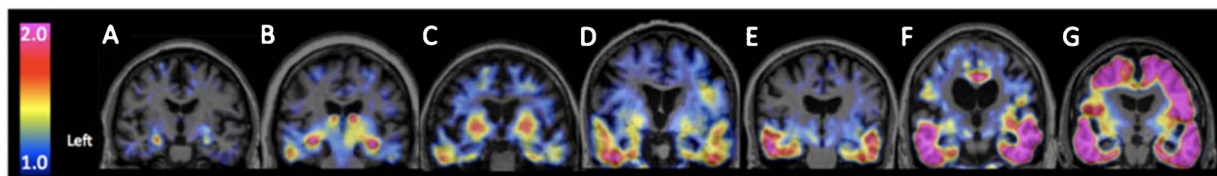
Tau PET radiotracers

Several tau PET tracers are now available in different stages of clinical development. The first tau tracer used in patients with AD, ^{18}F-FDDNP, suffered from a lack of selectivity as it binds to both amyloid-β and tau (Shoghi-Jadid et al. 2002). More-selective tracers that mainly aim to detect paired helical filament tau have since been developed. ^{11}C-PBB3 has been used to image AD and non-AD taoupathies but exhibited low specific binding, off-target binding, and a radiometabolite entering the brain (Kimura et al. 2015). New ^{18}F-derivatives are being developed, including [^{18}F] AM-PBB3 and [^{18}F]PM-PBB3, both recently evaluated in-humans. Initial results show improved performance in terms of broader dynamic range and less off-target binding around basal ganglia and thalamus (Ono et al. 2017a).

A series of tau tracers were developed at Tohoku University in Japan: ^{18}F-THK523, ^{18}F-THK5105, ^{18}F-THK5117, ^{18}F-THK5351 (Fodero-Tavoletti et al. 2010; Villemagne et al. 2014; Okamura et al. 2013; Stepanov et al. 2017; Betthauser et al. 2017). The first three of those tracers showed in human studies increased tracer uptake in AD patients compared to age-matched healthy controls in areas of the brain known to contain AD tauopathy, but also demonstrated high retention in white matter that precluded interpretation of the images through visual evaluation. The newest derivative in this family, ^{18}F-THK5351, shows faster kinetics, lower white matter retention and higher signal-to-noise ratio (Harada et al. 2015) (see Fig. 1). However, ^{18}F-THK5351 presents high levels of off-target binding to monoamine oxidase B (MAO-B) and therefore cannot be used to selectively detect tau pathology (Harada et al. 2017).

Pharmaceutical companies are developing tracers to support the advancement of novel therapies targeting tau. ^{18}F-AV-680 (formerly ^{18}F-T808) and ^{18}F-AV-1451
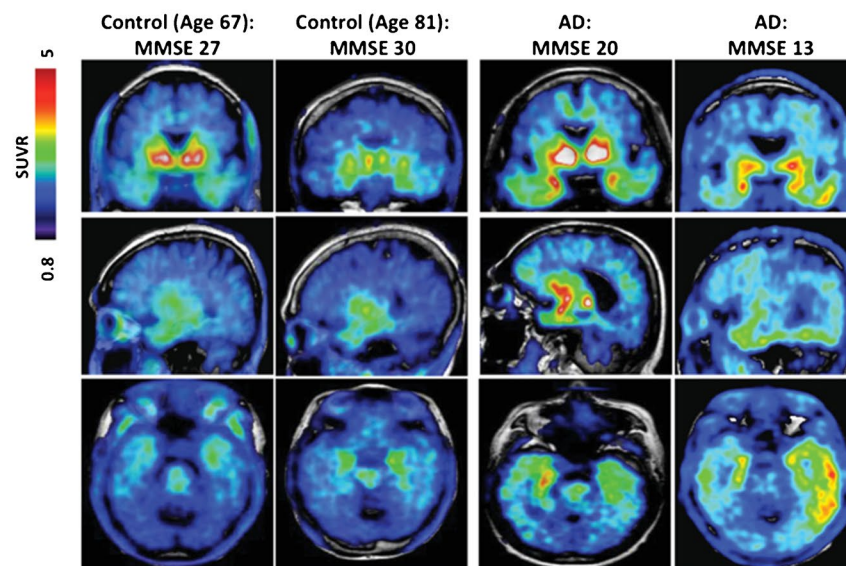

Fig. 1 Typical patterns of uptake observed with ^{18}F-AV-1451 and ^{18}F-THK5351. (1) (Adapted from Johnson et al. 2016) Coronal PET images of ^{18}F-AV-1451 80–100 min standardized-uptake-value-ratios (SUVR, with cerebellar reference) from 3 clinically normal (*A-C*), 2 mild cognitive impairment (*D, E*) and 2 mild Alzheimer dementia (*F, G*) participants. Cognitively impaired participants show elevated levels of cortical binding successively involving temporal, parietal, frontal, and occipital cortices. (2) (Adapted from Lockhart et al. 2016) Representative ^{18}F-THK5351 SUVR 40–60 min PET images of 4 participants (2 controls and 2 AD). These cases present different levels of binding that illustrate the dynamic range of SUVR across participants

(Flortaucipir, formerly ^{18}F-T807) were developed by Siemens and are now owned by Eli Lilly. Both show good pharmacokinetic properties, high binding affinity and good selectivity for tau over amyloid-β, but ^{18}F-AV-680 also shows moderate bone uptake (indicative of in-vivo defluorination) (Chien et al. 2013, 2014). ^{18}F-AV-1451 is the most widely used tau tracer to date. It has shown patterns of cortical retention comparable to known distributions of tau in AD, low retention in white matter, and a strong association with disease severity in AD (see Fig. 1). Despite the success of initial studies (Chien et al. 2013; Johnson et al. 2016; Schöll et al. 2016), ^{18}F-AV-1451 presents some drawbacks. First, reliable quantification is challenging, as the specific signal continues to increase through the duration of the PET scan in high-binding AD patients (see "Pharmacokinetic modeling" section) and, second, it presents off-target binding (i.e., binds to substances in the brain other than tau such as melanin and hemorrhage metabolites (Marquié et al. 2015)). These issues cloud the interpretation of longitudinal changes, as explained in more detail below.

These drawbacks prompted continued development of tau tracers with improved characteristics and several are now available and under investigation. The preclinical evaluations of these newer tracers report high affinity, selectivity and specificity. However, it is important to note that the methods vary across studies and, at this time, some results have been published only as preliminary conference abstracts (see Table 1). Preliminary clinical evaluations are also promising. ^{18}F-RO6958948, developed by Roche, has shown significantly higher uptake in AD patients compared to controls, lack of radiometabolites entering brain and no defluorination; clinical studies are ongoing (Wong et al. 2015). ^{18}F-GTP1, developed by Genentech, is under evaluation in a longitudinal natural history study. Preliminary cross-sectional results show an association between ^{18}F-GTP1 uptake and cognitive deficits in AD, but also notable off-target binding in basal ganglia (Sanabria-Bohorquez et al. 2016, 2017). Preliminary human results for a third tracer, ^{18}F-PI-2620, developed by Piramal Imaging, show robust uptake and fast wash-out in AD subjects, and focal asymmetric uptake in AD tau-bearing areas. Importantly, the preclinical characterization of ^{18}F-PI-2620 has shown evidence of strong binding in two non-AD tauopathies: Pick's (3R) and PSP (4R); a clinical study including PSP subjects is ongoing (Barret et al. 2017; Alzforum 2017). Finally, preliminary human studies for ^{18}F-MK-6240, developed by Merck, show desirable in-vivo kinetics, a large dynamic SUVR range, significant binding in areas known to contain AD tauopathy, and correlation between uptake and clinical endpoints (Sur et al. 2017; Salinas et al. 2017) (see Fig. 2). Human ^{18}F-MK-6240 studies are underway at several centers across the world.

Despite the encouraging results, more cross-sectional and longitudinal data are needed to fully evaluate the potential of each of these tracers to accurately characterize the pathological burden of low- and high-tau expressing brain regions and as AD biomarkers.

Status of "validation" of individual radiotracers

Generally, when a PET tracer is developed, an extensive validation that includes the precise determination of performance criteria such as binding selectivity and in-vivo pharmacokinetics (in "Pharmacokinetic modeling" section) is performed before its widespread use in human studies (Gunn et al. 2015). However, tau PET tracers are entering clinical trials whilst their validation is still ongoing, mainly motivated by the increasing disease burden and the pressuring need of finding effective treatments.

The binding selectivity of tau PET tracers can be characterized in-vitro through the comparison of immmunostained binding assays and autoradiography of postmortem brain slices of individuals diagnosed with AD. Autoradiographic evaluations of ^{18}F-AV-1451 have been strongly and consistently associated with classic tau deposition as confirmed both with immunohistochemistry cytoarchitecture and microscopy, and have not shown binding in neocortex from normal subjects, nor in cerebellar tissue from any source. Moreover, ^{18}F-AV-1451 studies have provided a conceptual basis for understanding how different tau tracers may detect different tauopathies, as its binding is more indicative of paired helical filament tau and not straight filament tau. In-vitro studies have been instrumental in the identification of ^{18}F-AV-1451 off-target binding to various substances such as melanin-containing cells, brain hemorrhagic lesions, iron-associated regions, substantia nigra, and calcifications in the choroid plexus (Marquié et al. 2015; Lowe et al. 2016; Ikonomovic et al. 2016; Lee et al. 2017). ^{18}F-AV-1451 has also been shown to bind with low affinity to monoamine oxidase A (MAO-A) (Vermeiren et al. 2015; Hostetler et al. 2016). Studies of ^{18}F-THK5351 have shown high levels of binding to MAO-B, suggesting limited utility for selective detection of tau pathology (Harada et al. 2017).

The in-vivo binding selectivity of tau PET tracers has to be characterized indirectly because competition and displacement studies, generally used in the development of radiotracers for receptors and other proteins, are not feasible as the high concentration of tau would require micromolar concentrations of the non-radioactive compound, most likely with toxic effects. Binding selectivity is determined in clinical studies by evaluating whether the tracer distribution differs in AD patients with respect to controls, follows the expected distribution of tau in AD based on postmortem studies, differs from that of other β-pleated sheet tracers, such as ^{11}C-PiB, and the extent to which tracer uptake

Table 1 Preclinical and in-vivo properties of tau PET tracers. IC_{50}: half-maximal inhibitory concentration; K_d: dissociation constant; ARG: determined by autoradiography; Ref: region of reference; CER: cerebellum; PSP: progressive supranuclear palsy; CBD: corticobasal degeneration; CTE: chronic traumatic encephalopathy; † Conference abstract

Radiotracer	Affinity	SUVR in AD tau-rich areas (min post-injection)	Reported off-target binding? (region or substrate-specific binding)	Off-target binding to MAO-A or MAO-B?	Binding to non-AD tauopathy?	References
11C-PBB3	K_d =2.5 nM in NFT-rich AD brain tissue Method: ARG	0.75–1.6 (30–70 min) Ref.: CER	Yes Dural venous sinuses, basal ganglia, thalamus	Not reported	Yes PSP, CBD, and Pick's disease	Maruyama et al. 2013; Kimura et al. 2015; Ono et al. 2017a, b
18F-THK5351	K_d =2.9 nM in hippocampal AD brain homogenates Method: in-vitro saturation binding	1.7–2.5 (50–60 min) Ref.: CER gray	Yes Basal ganglia (including striatum and substantia nigra), thalamus, midbrain, and periaqueductal gray matter	Yes very high affinity to MAO-B	Yes PSP and CBD	Harada et al. 2015, 2017; Betthauser et al. 2017
18F-AV-1451	Various values reported [1] K_d =14.6 nM in AD brain sections Method: ARG, saturation binding studies (Xia et al., 2013) [2] K_d =1.4–3.72 nM (enthorhinal cortex) K_d =0.63–1.70 nM (frontal cortex) in NFT-rich AD brain homogenates Method: saturation binding studies (Hostetler et al. 2016)	1–4 (80–100 min) Ref.: CER gray	Yes Basal ganglia (including striatum and substantia nigra), choroid plexus, midbrain, meninges, scalp Binds to: melanin-containing cells, leptomeningeal melanin, vessels, brain hemorrhagic lesions, iron-associated regions and calcifications	Yes low affinity to MAO-A; mixed results for MAO-B	No (evaluated in PSP, CBD, MAPT P301L mutation, Pick's disease, and CTE)	Xia et al. 2013; Vermeiren et al. 2015; Marquie et al. 2015, 2017, 2018; Ikonomovic et al. 2016; Lowe et al. 2016; Hostetler et al. 2016; Lee et al. 2017†; Lemoine et al. 2017†; Hansen et al. 2017
18F-RO6958948	IC_{50} =18.5 nM in late AD brain tissue (Braak V-VI) Method: ARG, displacement of [3H] T808	1–3 (60–90 min) Ref.: CER gray	None reported	No	No (evaluated in Pick's disease, PSP, and CBD)	Honer et al. 2017; Wong et al. 2015†
18F-GTP1	binding affinity: 14.9±0.43 nM in tau-positive brain tissue Method: ARG	1–3 (90–120 min) Ref: CER gray	In some subjects, signal in basal ganglia (may be non-tau age-related)	No	Not reported	Marik et al. 2016†; Sanabria-Bohorquez et al. 2016†; Alzforum 2017
18F-PI-2620	IC_{50} =1.8 nM in AD brain tissue Method: competition-assays	2.5–2.8 (90–100 min)	None reported	No	Yes Pick's disease and PSP	Mueller et al. 2017†; Barret et al. 2017†

Table 1 (continued)

Radiotracer	Affinity	SUVR in AD tau-rich areas (min post-injection)	Reported off-target binding? (region or substrate-specific binding)	Off-target binding to MAO-A or MAO-B?	Binding to non-AD tauopathy?	References
^{18}F-MK-6240	K_d ~0.3 nM in NFT-rich AD brain homogenates Method: saturation binding studies	2.5-4 (90–120 min)	Left leptomeningeal region, nasal sinus and red nucleus, meninges, superior anterior vermis, and focal hemangiomas	No	Unlikely (binds to same site as AV-1451)	Walji et al. 2016; Hostetler et al., 2016; Alzforum 2017; Betthauser et al. 2018[+]

measures relate to clinical variables, such as cognitive decline or neurodegeneration (Villemagne et al. 2015).

The gold standard validation of a PET tau tracer requires the comparison of in-vivo tracer uptake measured by PET and post-mortem measurements of tau concentration for the same individual. Although data collection for these studies is difficult and slow, some have been reported. ^{18}F-THK5351 binding was evaluated in brain samples from an autopsy-confirmed AD case who underwent ^{18}F-THK5351 PET months before death. In this study, Harada et al. (2017) confirmed that neocortical ^{18}F-THK5351 signal correlates with tau pathology but also with MAO-B levels in the brain, concluding that in-vivo ^{18}F-THK5351 signal likely reflects the combination of tau pathology and reactive astrocytes, and therefore has limited utility for selective detection of tau pathology. Following similar approaches, ^{18}F-AV-1451 was evaluated by two groups. Marquié et al. (2017) evaluated autopsy-confirmed non-AD tauopathy cases characterized by tau inclusions mainly composed of straight filaments (two PSP cases and a MAPT P301L mutation carrier), showing that ^{18}F-AV-1451 did not significantly correlate with tau deposits present in non-AD tauopathies and confirming off-target binding in neuromelanin-containing neurons in the substantia nigra. In another study, Smith et al. (2016) performed a neuropathological examination of a patient carrying the MAPT R406W mutation (produces the accumulation of tau tangles similar to those in AD) providing results that strongly support the notion that in-vivo ^{18}F-AV-1451 PET reflects the intensity of AD-type regional tau neuropathology.

Status of comparative evaluation across radiotracers

Existing tau PET tracers belong to different chemotype classes and present different binding properties. Direct comparisons across tracers in the same individual facilitate the evaluation of relative tracer performance, including differences that may affect the accuracy of visual interpretation and the sensitivity to subtle changes in tau loads over time.

Recent studies have reported preliminary comparisons of the in-vitro binding properties across different tau tracers. Lemoine et al. (2017) compared ^{18}F-THK5117 and ^{18}F-THK5351 to ^{11}C-PBB3 and to ^{18}F-AV-1451 in autopsy brains of AD patients, concluding that the three different families show different binding properties that likely reflect different binding sites on tau. Ono et al. (2017b) compared ^{11}C-PBB3 and ^{18}F-AV-1451 using tauopathy brain samples, showing distinct selectivity of ^{11}C-PBB3 for diverse tau fibril strains, and concluding that ^{11}C-PBB3 has a superior ability to capture wide-range tauopathies. Lowe et al. (2017) compared ^{18}F-THK5351 to ^{18}F-AV-1451 in a wide range of pathologies, observing reduced binding of ^{18}F-THK5351 compared to ^{18}F-AV-1451 in some AD cases,

Fig. 2 Patterns of uptake observed with ^{18}F-MK6240 in a healthy volunteer (HV) and three subjects with AD at different disease stages. ^{18}F-MK6240 uptake levels and extent increase with disease severity. Courtesy of Cristian Salinas, Biogen
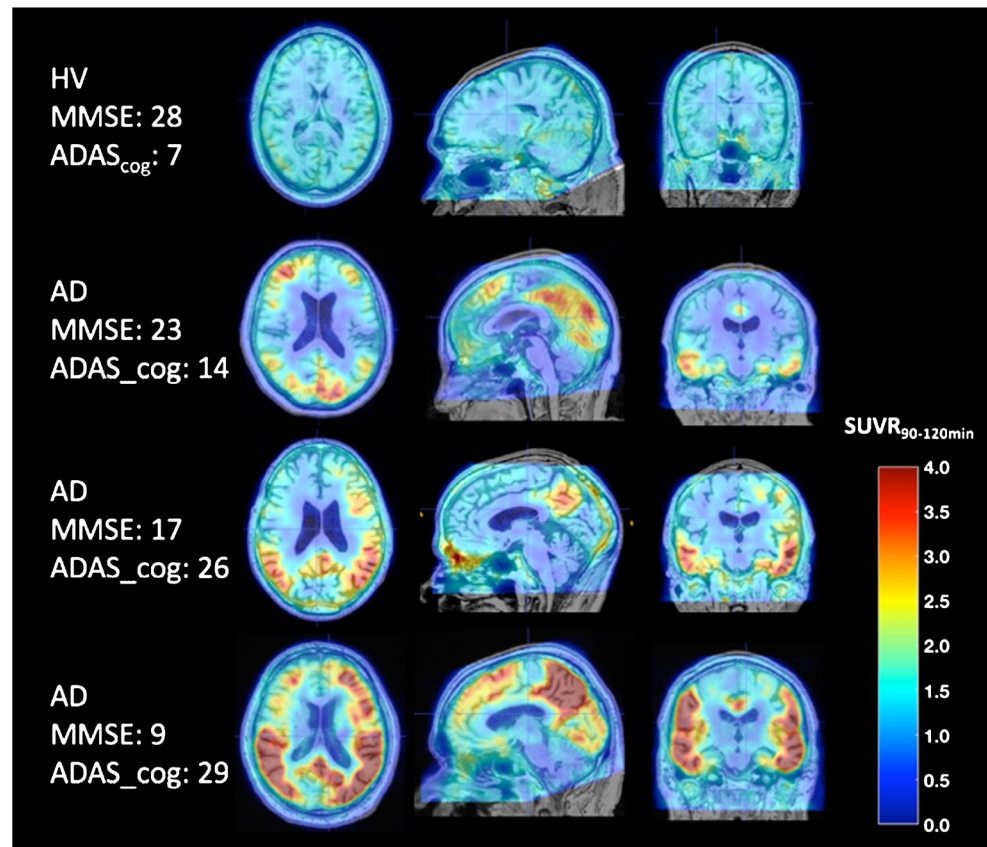
and concluding that ^{18}F-THK5351 may yield lower signal in AD clinical imaging. Lowe et al. (2017) also observed off-target sites common for both tracers, but noted additional ^{18}F-THK5351 off-target binding, which may increase the likelihood of falsely mimicking tau pathology.

Preliminary results on in-vivo head-to-head tracer comparisons have recently been presented. Chiotis et al. (2017) compared ^{18}F-THK5351 and ^{11}C-PBB3 in a group of patients with AD. Both tracers showed binding in the temporal lobes and other isocortical areas, although ^{18}F-THK5351 presented greater grey matter binding. Distinct off-target binding areas were identified for each tracer. Similarly, Jang et al. (2017) compared ^{18}F-AV-1451 and ^{18}F-THK5351 in various neurodegenerative diseases, concluding that ^{18}F-AV-1451 is more specific to AD and less likely to present off-target binding, while ^{18}F-THK5351 is more likely to reflect non-specific neurodegeneration. These findings generally agree with the in-vitro observations described above.

Pharmacokinetic modeling

The characterization of a novel tau PET tracer requires evaluation of its in-vivo kinetic properties, such as: metabolism of the radiotracer in plasma and evaluation of radiolabeled metabolites; sensitivity of radiotracer binding measure to variations in blood flow; accuracy, precision and temporal stability of non-specific and specific binding outcomes, including test/retest variability; and capacity of binding measure to distinguish subject groups. Quantification is needed to understand nonspecific and off-target tracer uptake, to identify reference regions offering robust quantification of target uptake and ranking of uptake values, and to understand the impact of varying levels of cerebral atrophy and neurodegeneration on data interpretation.

Full kinetic modeling evaluations (with arterial blood sampling) entail, however, significant subject burden. It is therefore common to use simplified methods, such as ratios of the uptake in the target region to that in a nonspecific reference region (standardized-uptake-value ratio, SUVR). The SUVR is a simple and feasible index that has proven useful for assessment of amyloid-β and tau PET load, as it is generally associated with low measurement variability and power for discriminating high- from low-signal. Although the SUVR is practical to apply, it provides a biased estimate of amyloid-β or tau load relative to quantitative outcomes (Slifstein 2008; Carson et al. 1993). While this bias may be acceptable, it remains a relevant issue for longitudinal imaging, early detection, and assessment of post-therapy change.

Most of the recent reports on kinetic evaluations of tau tracers focus on ^{18}F-AV-1451 (Shcherbinin et al. 2016; Barret et al. 2016; Baker et al. 2016; Wooten et al. 2016; Hahn et al. 2017). The quantitative results support late SUVR

measures (80–100 or 75–105 min), with a few significant observations. First, ^{18}F-AV-1451 SUVR time-activity curves can exhibit steady accumulation for high-binders (e.g., SUVR > 1.5) as late as 150–210 min post-injection. In contrast, an earlier plateau (80–100 min) is observed for low binders, who are most relevant for early disease detection. Second, different kinetics are observed in off-target areas that may confound quantification in adjacent target regions. Third, distribution volume (V_T) measures successively decrease from AD to older controls to young controls for all regions, including nonspecific cerebellar retention (Barret et al. 2016). Fourth, age-related dependence in V_T suggests importance of age-matching between controls and patients (Barret et al. 2016). The impact of the latter two factors is somewhat mitigated by the use of SUVR or BP_{ND}. However, the lack of SUVR plateau for high binding areas requires precise SUVR acquisition time across longitudinal assessments to minimize this source of unwanted bias.

As the stability and accuracy of the SUVR depends on the extent to which underlying assumptions are violated, and that may vary over time (e.g., radiotracer delivery or clearance in target and reference regions (Slifstein 2008)), in-vivo kinetic modeling evaluations should be performed in enough subjects (~ 20) to represent the dynamic PET signal range and to study nonspecific binding, in order to understand SUVR changes across cross-sectional cohorts or longitudinally for a given individual.

Additional methodological considerations

The anatomic distribution of retention of tau tracers, particularly in early stages of age- and AD- related tauopathy, is variable within vulnerable areas and often bilaterally asymmetric. These characteristics pose a challenge for standardization of measures that capture both tau deposit burden and locale. The relative superiority of global, i.e., pancerebral, measures versus regional, i.e., anatomic ROI measurements, has not been rigorously established for tau.

The spatial extent of pathologically verified AD tauopathy is substantially greater (due to its neocortical involvement) than the more benign tauopathy of aging (confined to the more primitive cortex of the medial temporal lobe). These processes may largely share a pathogenesis (Duyckaerts et al. 2015; Crary et al. 2014), but AD includes markedly elevated amyloid-β deposition as well as neocortical tau deposition. PET thus may be useful for distinguishing these tauopathies on the basis of anatomic burden. However, Braak Stage 0 (absence of tauopathy) will not be reliably distinguished from Stage I (age-related, early tauopathy in medial temporal lobe) with current PET sensitivity.

Different approaches are being pursued to improve tau PET utility for detecting early pathology, for example, the use of individualized "pathological volumes" defined in comparison to normal controls or weighted neocortical ROIs selected to show maximal diagnostic group separation (Abdi et al. 2012). A recent study evaluated multiple whole-brain and region-specific approaches to detect clinically relevant tau PET signal, suggesting that whole-brain tau PET measures might be adequate biomarkers to detect AD-related tau pathology, although regional measures in AD-vulnerable regions may increase sensitivity to early tau PET signal, atrophy, and memory decline (Maass et al. 2017). The definition of ROIs in longitudinal studies includes yet another layer of complexity, as it is still under debate what is most relevant to follow progression over time (i.e., intensity of tau tracer signal, extent of tracer distribution, or both) (Devous et al. 2015). An initial investigation on the rate of change of tau binding uses a surface-based cluster approach (Becker et al. 2017).

Amyloid-β load is often evaluated as a dichotomous variable and used for classification of subjects with respect to a pre-defined positivity threshold. More recently, intermediate rather than high levels of amyloid-β burden have been used as inclusion criteria for observational and clinical AD prevention studies (Landau 2016). Recent tau studies have followed this approach, using thresholds for the classification of subjects with abnormal tau tracer retention in selected ROIs (e.g., studies with ^{18}F-AV-1451 aimed at recapitulating Braak histopathological stages (Schwarz et al. 2016)). However, the treatment of tau load as a continuous variable may provide crucial information, particularly given the close association of regional tau load with cognitive decline (Hanseeuw et al. 2017; Mormino et al. 2017).

Although PET may provide a unique tool for the evaluation of potential disease-modifying treatments, results should be interpreted with caution, as much of the actual toxic effect of tau and amyloid-β fragments may occur at levels not detectable with PET. Thus, the deposited forms of AD pathology may represent a sequestration of toxic species that is temporally removed from the toxic event and may be asynchronous with a therapeutic drug effect.

Conclusion

We have witnessed a tremendous advance in the development of selective tau PET tracers in recent years, which provide a unique opportunity to advance our understanding of AD and to follow the relationship between tau and amyloid-β over time. Tau load is a promising potential candidate as biomarker of disease progression, given the close association with cognitive decline. In this paper we reviewed the recent developments in tau PET imaging from a methodological perspective. Tau tracers are entering clinical trials and providing interesting results, whilst their validation is being performed in parallel.

Despite some encouraging results, more data is needed to fully determine the usefulness of tau tracers for characterizing the pathological burden of low and high tau-expressing brain regions and as biomarkers for AD and other tauopathies.

Compliance with ethical standards

Ethical approval This article does not contain any studies with human participants or animals performed by any of the authors.

Conflict of interest CL and IG declare no conflict of interest. KAJ reports grants from NIH, Fidelity Biosciences, Harvard Neurodiscovery Center, and from the Alzheimer's Association; and consulting for Lilly/Avid, Piramal, Abbvie, Biogen, Janssen, Merck, Novartis, Genentech and GEHC. JCP reports NIH grant R01 AG050436; speaker honoraria from Yale University, Mount Sinai Hospital and Georgetown University; and is a member of NIH Center for Scientific Review Advisory Council.

References

Abdi, H., Williams, L., Beaton, D., Posamentier, M., Harris, T., Krishnan, A., et al. (2012). Analysis of regional cerebral blood flow data to discriminate among Alzheimer's disease, frontotemporal dementia, and elderly controls: a multi-block barycentric discriminant analysis (MUBADA) methodology. *Journal Alzheimers Diseases, 31*(S3), S189-201.

Alzforum networking for a cure, News April 2017. (http://www.alzforum.org/news/conference-coverage/next-generation-tau-pet-tracers-strut-their-stuff).

Alzheimer's Association. (2015). Changing the Trajectory of Alzheimer's Disease: How a Treatment by 2025 Saves Lives and Dollars, Alzheimer's Association report. http://www.alz.org/documents custom/trajectory.pdf.

Alzheimer's Association. (2016). 2016 Alzheimer's disease facts and figures. *Alzheimer's & Dementia, 12*(4), 459–509.

Arriagada, P. V., Growdon, J. H., Hedley-Whyte, E. T., & Hyman, B. T. (1992). Neurofibrillary tangles but not senile plaques parallel duration and severity of Alzheimer's disease. *Neurology, 42*(3), 631–631.

Baker, S. L., Lockhart, S. N., Price, J. C., He, M., Huesman, R. H., Schonhaut, D., et al. (2016). Reference tissue–based kinetic evaluation of 18 F-AV-1451 for tau imaging. *Journal of Nuclear Medicine, 58*(2), 332–338.

Barret, O., Alagille, D., Sanabria, S., Comley, R. A., Weimer, R. M., Borroni, E., et al. (2016). Kinetic modeling of the tau PET tracer 18F- AV-1451 in human healthy volunteers and alzheimer's disease subjects. *Journal of Nuclear Medicine, 58*(7), 1124–1131.

Barret, O., Seibly, J., Stephens, A., Madonia, J., Alagille, D., Mueller, A., et al. (2017). Initial clinical PET studies with the novel tau agent 18-F PI-2620 in Alzheimer's disease and controls. *Journal of Nuclear Medicine, 58*(Suppl 1), 630.

Becker, J. A., Cosio, D., Lee, C., Andrea, N., Sperling, R., & Johnson, K. (2017). A cortical cluster-based measure of change in longitudinal 18F-T807 FTP PET. Human Amyloid Imaging, *Conference abstract.*

Betthauser, T. J., Lao, P. J., Murali, D., Barnhart, T. E., et al. (2017). In vivo comparison of tau radioligands 18F-THK-5351 and 18F-THK-5317. *Journal of Nuclear Medicine, 58*(6), 996–1002.

Betthauser, T. J., Murali, D., Barnhart, T., Stone, C., et al. (2018). In vivo observations and quantification of tau with [F-18] MK-6240 PET from young controls to Alzheimer's disease. Human Amyloid Imaging, *Conference abstract.*

Bierer, L. M., Hof, P. R., Purohit, D. P., Carlin, L., Schmeidler, J., Davis, K. L., et al. (1995). Neocortical neurofibrillary tangles correlate with dementia severity in alzheimer's disease. *Archives of Neurology, 52*(1), 81–88.

Braak, H., & Braak, E. (1991). Neuropathological stageing of Alzheimer-related changes. *Acta Neuropathologica, 82*(4), 239–259.

Braak, H., & Braak, E. (1999). Temporal sequence of Alzheimer's disease-related pathology. In A. Peters, J. H. Morrison (Eds.), Cerebral Cortex (vol 14 pp. 475–512). Boston: Springer.

Braak, H., Thal, D. R., Ghebremedhin, E., & Del Tredici, K. (2011). Stages of the pathologic process in alzheimer disease: age categories from 1 to 100 Years. *Journal of Neuropathology & Experimental Neurology, 70*(11), 960–969.

Carson, R. E., Channing, M. A., Blasberg, R. G., Dunn, B. B., Cohen, R. M., Rice, K. C., & Herscovitch, P. (1993). Comparison of bolus and infusion methods for receptor quantitation: application to 18F-cyclofoxy and positron emission tomography. *Journal of Cerebral Blood Flow and Metabolism, 13*, 24–42.

Chien, D., Bahri, S., Szardenings, A., Walsh, J., Mu, F., Su, M., et al. (2013). Early clinical PET imaging results with the novel PHF-tau radioligand [F-18]-T807. *Journal of Alzheimers Disease, 34*, 457–68.

Chien, D., Szardenings, A., Bahri, S., Walsh, J., Mu, F., Xia, C., et al. (2014). Early clinical PET imaging results with the novel PHF-tau radioligand [F18]-T808. *Journal of Alzheimers Disease, 38*, 171–84.

Chiotis, K., Stenkrona, P., Almkvist, O., Arakawa, R., Takano, A., Stepanov, V., et al. (2017). Head-to-head comparison of tau-specific tracers in Alzheimer's disease: [11C]THK5351 vs [11C]PBB3 PET imaging. Human Amyloid Imaging, *Conference abstract.*

Cho, H., Choi, J. Y., Hwang, M. S., Kim, Y. J., Lee, H. M., Lee, H. S., Lee, J. H., Ryu, Y. H., Lee, M. S., & Lyoo, C. H. (2016). In vivo cortical spreading pattern of tau and amyloid in the Alzheimer disease spectrum. *Annals of Neurology, 80*(2), 247–258.

Crary, J., Trojanowski, J., Schneider, J., Abisambra, J., Abner, E., Alafuzoff, I., et al. (2014). Primary age-related tauopathy (PART): a common pathology associated with human aging. *Acta Neuropathologica, 128*, 755–66.

Dani, M., Brooks, D., & Edison, P. (2016). Tau imaging in neurodegener- ative diseases. *European Journal Nuclear Medicine and Molecular Imaging, 43*, 1139–1150.

Delacourte, A., David, J. P., Sergeant, N., Buee, L., Wattez, A., Vermersch, P., et al. (1999). The biochemical pathway of neurofibrillary degeneration in aging and Alzheimer's disease. *Neurology, 52*(6), 1158–1158.

Devous, M. D., Joshi, A. D., Navitsky, M., Kennedy, I., Lu, M., Pontecorvo, M. J., et al. (2015). Understanding the topology of 18F-AV-1451 (also known as T807) PET tau images in Alzheimer's disease. *Alzheimer's & Dementia, 11*(7), 283–284.

Donohue, M. C., Sperling, R. A., Petersen, R., Sun, C.-K., Weiner, M. W., & and, P. S. A (2017). Association Between Elevated Brain Amyloid and Subsequent Cognitive Decline Among Cognitively Normal Persons. *JAMA, 317*(22), 2305.

Drachman, D. A. (2014). The amyloid hypothesis time to move on: Amyloid is the downstream result, not cause, of Alzheimer's disease. *Alzheimer's & Dementia, 10*(3), 372–380.

Duyckaerts, C., Braak, H., Brion, J., Buee, L., Del, T. K., Goedert, M., et al. (2015). PART is part of Alzheimer disease. *Acta Neuropathologica, 129*, 749–56.

EXPEDITION 3 -Progress of Mild Alzheimer's Disease in Participants on Solanezumab Versus Placebo. https://clinicaltrials.gov/ct2/show/study/NCT01900665.

Fessel, J. (2018) Amyloid is essential but insufficient for Alzheimer causation: addition of subcellular cofactors is required for dementia. *International Journal of Geriatric Psychiatry, 33*, 14–21.

Fodero-Tavoletti, M. T., Okamura, N., Mulligan, R., Furumoto, S., Connor, A. R., Kudo, Y., et al. (2010). Characterisation of [18F]-THK523 a novel in vivo tau imaging ligand. *Alzheimer's & Dementia, 6*(4), S432.

Giacobini, E., & Gold, G. (2013). Alzheimer disease therapy: moving from amyloid-β to tau. *Nature Reviews Neurology, 9*(12), 677–686.

Goate, A., Chartier-Harlin, M., Mullan, M., Brown, J., Crawford, F., Fidani, L., et al. (1991). Segregation of a missense mutation in the amyloid precursor protein gene with familial Alzheimer's disease. *Nature, 349*, 704–706.

Gunn, R. N., Slifstein, M., Searle, G. E., & Price, J. C. (2015). Quantitative imaging of protein targets in the human brain with PET. *Physics in Medicine and Biology, 60*(22), R363–R411.

Hahn, A., Schain, M., Erlandsson, M., Sjolin, P., James, G., Strandberg, O., et al. (2017). Modeling strategies for quantification of in vivo 18F- AV1451 binding in patients with tau pathology. *Journal of Nuclear Medicine, 58*(4), 623–631.

Hanseeuw, B. J., Betensky, R. A., Schultz, A. P., Papp, K. V., Mormino, E. C., Sepulcre, J., et al. (2017). Fluorodeoxyglucose metabolism associated with tau-amyloid interaction predicts memory decline. *Annals of Neurology, 81*(4), 583–596.

Hansen, A. K., Brooks, D. J., & Borghammer, P. (2017). MAO-B Inhibitors do not block. in vivo Flortaucipir([18F]-AV-1451) binding. *Molecular Imaging Biology*. https://doi.org/10.1007/s11307-017-1143-1.

Harada, R., Ishiki, A., Kai, H., Sato, N., Furukawa, K., Furumoto, S., Tago, T., et al. (2017). Correlations of 18F-THK5351 PET with post-mortem burden of tau and astrogliosis in Alzheimer's disease. *Journal of Nuclear Medicine*. https://doi.org/10.2967/jnumed.117.197426.

Harada, R., Okamura, N., Furumoto, S., Furukawa, K., Ishiki, A., Tomita, N., et al. (2015). 18F-THK5351: a novel PET radiotracer for imaging neurofibrillary pathology in Alzheimer disease. *Journal of Nuclear Medicine, 57*(2), 208–214.

Harada, R., Okamura, N., Furumoto, S., Tago, T., Yanai, K., Arai, H., et al. (2016). Characteristics of Tau and Its Ligands in PET Imaging. *Biomolecules, 6*(1), 7.

Hardy, J. (2002). The amyloid hypothesis of alzheimer's disease: progress and problems on the road to therapeutics. *Science, 297*(5580), 353–356.

Harrison, J., & Owen, M. (2016). Alzheimer's disease: the amyloid hypothesis on trial. *British Journal Psychiatry, 208*, 1–3.

Heneka, M., Carson, M., El, K. J., Landreth, G., Brosseron, F., Feinstein, D., et al. (2015). Neuroinflammation in Alzheimer's disease. *Lancet Neurology, 14*, 388–405.

Herrup, K. (2015). The case for rejecting the amyloid cascade hypothesis. *Nature Neuroscience, 18*(6), 794–799.

Honer, M., Gobbi, L., Knust, H., Kuwabara, H., Muri, D., et al. (2017). Preclinical evaluation of (18)F-RO6958948, (11)C-RO6931643 and (11)C-RO6924963 as novel radiotracers for imaging aggregated tau in AD with positron emission tomography. *Journal Nuclear Medicine*. https://doi.org/10.2967/jnumed.117.196741.

Hostetler, E., Walji, A., Zeng, Z., Miller, P., Bennacef, I., Salinas, C., et al. (2016). Preclinical characterization of 18F-MK-6240, a promising PET tracer for in vivo quantification of human neurofibrillary tangles. *Journal of Nuclear Medicine, 57*(10), 1599–1606.

Hyman, B. T., Phelps, C. H., Beach, T. G., Bigio, E. H., Cairns, N. J., Carrillo, M. C., et al. (2012). National Institute on Aging–Alzheimer's Association guidelines for the neuropathologic assessment of Alzheimer's disease. *Alzheimer's & Dementia, 8*(1), 1–13.

Ikonomovic, M. D., Abrahamson, E. E., Price, J. C., Mathis, C. A., & Klunk, W. E. (2016). [F-18]AV-1451 PET retention in the choroid plexus: more than "off-target" binding. *Annals of Neurology, 80*(2), 307–308.

Jang, Y., Lyoo, C. H., Park, S., et al. (2017). Head to head comparison of [18F] AV-1451 and [18F] THK5351 for tau imaging in Alzheimer's disease and frontotemporal dementia. *European Journal Nuclear Medicine Molecular Imaging (2017)*. https://doi.org/10.1007/s00259-017-3876-0.

Johnson, K. A., Schultz, A., Betensky, R. A., Becker, J. A., Sepulcre, J., Rentz, D., et al. (2016). Tau positron emission tomographic imaging in aging and early Alzheimer disease. *Annals of Neurology, 79*(1), 110–119.

Jonsson, T., Atwal, J., Steinberg, S., Snaedal, J., Jonsson, P., Bjornsson, S., et al. (2012). A mutation in APP protects against Alzheimer's disease and age-related cognitive decline. *Nature, 488*, 96 – 9.

Kimura, Y., Ichise, M., Ito, H., Shimada, H., Ikoma, Y., Seki, C., et al. (2015). PET Quantification of Tau Pathology in Human Brain with 11C- PBB3. *Journal of Nuclear Medicine, 56*(9), 1359–1365.

Klunk, W. E., Engler, H., Nordberg, A., Wang, Y., Blomqvist, G., Holt, D. P., Bergström, M., et al. (2004). Imaging brain amyloid in Alzheimer's disease using the novel PET tracer, PIB. *Annals of Neurology, 55*, 306–319.

Landau, S. (2016). The clinical significance of increasing amyloid in cognitively normal, amyloid negative individuals. Human Amyloid Imaging, *Conference abstract.*

Lee, C., Marquie, M., Andrea, N., LaPoint, M., Jin, D., Jacobs, H., et al. (2017). 18F Flortaucipir binding in choroid plexus: association with race and hippocampus binding. Human Amyloid Imaging, *Conference abstract.*

Lemoine, L., Gillberg, P., Svedberg, M., Stepanov, V., Jia, Z., Huang, J., Nag, S., Tian, H., et al. (2017). Comparative binding properties of the tau PET tracers THK5117, THK5351, PBB3, and T807 in postmortem Alzheimer brains. *Alzheimers Research & Theraphy, 9*(1), 96.

Liu, F., & Gong, C. X. (2008). Tau exon 10 alternative splicing and tauopathies. *Molecular Neurodegeneration, 3*(1), 8.

Lockhart, S. N., Baker, S., Okamura, N., Furukawa, K., Ishiki, A., Furumoto, S., et al. (2016). Dynamic PET measures of tau accumulation in cognitively normal older adults and Alzheimer's disease patients measured using [18F] THK-5351. *PLoS ONE, 11*(6), e0158460.

Lopresti, B. J., Klunk, W. E., Mathis, C. A., Hoge, J. A., Ziolko, S. K., Lu, X., Meltzer, C. C., et al.. Schimmel, K., Tsopelas, N. D., DeKosky, S. T., Price, J. C. (2005). Simplified quantification of Pittsburgh Compound B amyloid imaging PET studies: a comparative analysis. *Journal of Nuclear Medicine, 46*(12), 1959–1972.

Lowe, V., Curran, G., Fang, P., Liesinger, A., Josephs, K., Parisi, J., et al. (2016). An autoradiographic evaluation of AV-1451 Tau PET in dementia. *Acta Neuropathologica Communications, 4*, 58.

Lowe, V., Murray, M., Sarma, V., Curran, G., Fang, P., Pandey, M., et al. (2017). An autoradiographic evaluation of THK-5351 compared to AV-1451. Human Amyloid Imaging, *Conference abstract.*

Maass, A., Landau, S., Baker, S. L., Horng, A., Lockhart, S. N., La Joie, R., et al. (2017). Comparison of multiple tau-PET measures

as biomarkers in aging and Alzheimer's disease. *Neuroimage, 157*, 448–463.

Marik, J., Tinianow, J., Ogasawara, A., Liu, N., Williams, S., Lyssikatos, J., Barret, O., et al. (2016). [18F]GTP1 – A tau specific tracer for imaging tau-pathology in AD. Human Amyloid Imaging, *Conference abstract*.

Maruyama, M., Shimada, H., Suhara, T., Shinotoh, H., Ji, B., et al. (2013). Imaging of tau pathology in a tauopathy mouse model and in Alzheimer patients compared to normal controls. *Neuron, 79*(6), 1094-108. https://doi.org/10.1016/j.neuron.2013.07.037.

Marquie, M., Aguero, C., Siao Tick Chong, M., Ramanan, P., Saez-Calveras, N., et al. (2018). F-18]-AV-1451 binding profile in Chronic Traumatic Encephalopathy: a postmortem case series. Human Amyloid Imaging, *Conference abstract*.

Marquie, M., Normandin, M. D., Meltzer, A. C., Chong, M. S. T., Andrea, N. V., Anton-Fernandez, A., et al. (2017). Pathological correlations of [F-18]-AV-1451 imaging in non-alzheimer tauopathies. *Annals of Neurology, 81*(1), 117–128.

Marquie, M., Normandin, M. D., Vanderburg, C. R., Costantino, I. M., Bien, E. A., Rycyna, L. G., et al. (2015). Validating novel tau positron emission tomography tracer [F-18]-AV-1451 (T807) on postmortem brain tissue. *Annals of Neurology, 78*(5), 787–800.

Mathis, C. A., Klunk, W. E., Price, J. C., & DeKosky, S. T. (2005). Amyloid imaging with Pittsburgh Compound B. *Alzheimer's & Dementia, 1*(1), S6–S7.

Mintun, M. A., Larossa, G. N., Sheline, Y. I., Dence, C. S., Lee, S. Y., Mach, et al. (2006). [11C]PIB in a nondemented population: potential antecedent marker of Alzheimer disease. *Neurology, 67*, 446–452.

Mormino, E., Schultz, A., Papp, K., LaPoint, M., Hanseeuw, B., Hedden, T., et al. (2017). Neocortical Tau and hippocampus volume reflect distinct processes in preclinical Alzheimer's disease. *Alzheimer's & Dementia, 13*(7), S5–S6.

Mueller, A., Kroth, H., Berndt, M., Capotosti, F., Molette, J., Schieferstein, H., et al. (2017). Characterization of the novel PET tracer PI-2620 for the assessment of Tau pathology in Alzheimer's disease and other tauopathies. *Journal of Nuclear Medicine, 58*(Suppl.1), 847.

Ng, K. P., Pascoal, T. A., Mathotaarachchi, S., Therriault, J., Kang, M. S., Shin, M., et al. (2017). Monoamine oxidase B inhibitor, selegiline reduces 18F-THK5351 uptake in the human brain. *Alzheimers Res Ther, 9*(1), 25.

Okamura, N., Furumoto, S., Fodero-Tavoletti, M. T., Mulligan, R. S., Harada, R., Yates, P., et al. (2014). Non-invasive assessment of Alzheimer's disease neurofibrillary pathology using 18F-THK5105 PET. *Brain, 137* (6), 1762–1771.

Okamura, N., Furumoto, S., Harada, R., Tago, T., Yoshikawa, T., Fodero- Tavoletti, M., et al. (2013). Novel 18F-labeled arylquinoline derivatives for noninvasive imaging of tau pathology in Alzheimer disease. *Journal of Nuclear Medicine, 54*(8), 1420–1427.

Okamura, N., & Yanai, K. (2017). Brain imaging: applications of tau PET imaging. *Nature Reviews Neurology, 13*, 197–198.

Olson, M. I., & Shaw, C. M. (1969). Presenile dementia and Alzheimer's disease in mongolism. *Brain, 92*(1), 147–156.

Ono, M., Kitamura, S., Shimada, H., Sahara, N., Takuwa, H., Yoshiyama, Y., et al. (2017a). Development of novel tau PET tracers, [18F]AM-PBB3 and [18F]PM-PBB3. Human Amyloid Imaging, *Conference abstract*.

Ono, M., Sahara, N., Kumata, K., Ji, B., Ni, R., Koga, S., et al. (2017b). Distinct binding of PET ligands PBB3 and AV-1451 to tau fibril strains in neurodegenerative tauopathies. *Brain, 140*(3), 764–780.

Ossenkoppele, R., Schonhaut, D. R., Schöll, M., Lockhart, S. N., Ayakta, N., Baker, S. L., et al. (2016). Tau PET patterns mirror clinical and neuroanatomical variability in Alzheimer's disease. *Brain, 139*(5), 1551–1567.

Price, J. C., Klunk, W. E., Lopresti, B. J., Lu, X., Hoge, J. A., Ziolko, S. K., Holt, D. P., et al. (2005). Kinetic modeling of amyloid binding in humans using PET imaging and Pittsburgh Compound-B. *Journal of Cerebral Blood Flow & Metabolism, 25*, 1528–1547.

Saint-Aubert, L., Lemoine, L., Chiotis, K., Leuzy, A., Rodriguez-Vieitez, E., & Nordberg, A. (2017). Tau PET imaging: present and future directions. *Molecular Neurodegeneration, 12*, 19.

Salinas, C., Chiao, P., Purohit, A., Schmidt, K., Beaver, J., Sur, C., et al. (2017). Quantitative analysis and correlation with clinical endpoints of [18F]MK6240 targeting neurofibrillary tangles (NFTs) in healthy volunteers and subjects with Alzheimer's disease. Human Amyloid Imaging, *Conference abstract*.

Sanabria-Bohorquez, S., Barret, O., Tamagnan, G., Alagille, D., Marik, J., Ayalon, G., et al. (2016). Evaluation of Tau burden in a cross-sectional cohort of Alzheimer's disease subjects usign [18F]GTP1 (Genentech Tau Probe 1). *Alzheimer's & Dementia, 12*(7), P1172.

Sanabria-Bohorquez, S., Bentsson, T., Barret, O., Tamagnan, G., Alagille, D., de Crespigny, A., et al. (2017). Kinetics of [18F] GTP1 (Genentech tau probe 1) in the basal ganglia of Alzheimer's patients and healthy controls. Human Amyloid Imaging, *Conference abstract*.

Scholl, M., Lockhart, S., Schonhaut, D., O'Neil, J., Janabi, M., Ossenkoppele, R., et al. (2016). PET Imaging of tau deposition in the aging human brain. *Neuron, 89*, 971 – 82.

Schwarz, A. J., Yu, P., Miller, B. B., Shcherbinin, S., Dickson, J., Navitsky, M., et al. (2016). Regional profiles of the candidate tau PET ligand18F-AV-1451 recapitulate key features of Braak histopathological stages. *Brain, 139*(5), 1539–1550.

Selkoe, D., & Hardy, J. (2016). The amyloid hypothesis of Alzheimer's disease at 25 years. *EMBO Molecular Medicine, 8*, 595–608.

Shcherbinin, S., Schwarz, A. J., Joshi, A. D., Navitsky, M., Flitter, M., Shankle, W. M., Devous, M. D., & Mintun, M. A. (2016). Kinetics of the tau PET tracer 18F-AV-1451 (T807) in subjects with normal cognitive function, mild cognitive impairment, and Alzheimer disease. *Journal Nuclear Medicine, 57*(10), 1535–1542.

Shoghi-Jadid, K., Small, G. W., Agdeppa, E. D., Kepe, V., Ercoli, L. M., Siddarth, P., et al. (2002). Localization of neurofibrillary tangles and beta-amyloid plaques in the brains of living patients with alzheimer disease. *The American Journal of Geriatric Psychiatry, 10*(1), 24–35.

Slifstein, M. (2008). Revisiting an Old Issue: the Discrepancy Between Tissue Ratio-Derived Binding Parameters and Kinetic Modeling-Derived Parameters After a Bolus of the Serotonin Transporter Radioligand 123I- ADAM. *Journal of Nuclear Medicine, 49*(2), 176–178.

Smith, R., Puschmann, A., Scholl, M., Ohlsson, T., van Swieten, J., Honer, M., et al. (2016). 18F-AV-1451 tau PET imaging correlates strongly with tau neuropathology in MAPT mutation carriers. *Brain, 139*(9), 2372–2379.

Sperling, R., Mormino, E., & Johnson, K. (2014). The evolution of preclinical Alzheimer's disease: implications for prevention trials. *Neuron, 84*(3), 608–622.

Stepanov, V., Svedberg, M., Jia, Z., Krasikova, R., Lemoine, L., Okamura, N., et al. (2017). Development of [11C]/[3H]THK-5351 – a potential novel carbon-11 tau imaging PET radioligand. *Nuclear Medicine and Biology, 46*, 50–53.

Sur, C., Struyk, A., Bennacef, I., Lohith, T., Salinas, C. A., Telan-Choing, F., et al. (2017). [18F]MK-6240, a novel neurofibrillary tangles PET tracer: evaluation in healthy subjects and Alzheimer's disease patients. Human Amyloid Imaging, *Conference abstract*.

Vermeiren, C., Mercier, J., Viot, D., Mairet-Coello, G., Hannestad, J., Courade, J.-P., et al. (2015). T807 a reported selective tau tracer, binds with nanomolar affinity to monoamine oxidase A. *Alzheimer's & Dementia, 11*(7), P283.

Villemagne, V., Rowe, C., Tamagnan, G., Fodero-Tavoletti, M., Oka-
    mura, N., Furumoto, S., et al. (2014). In vivo tau imaging with
    18F- THK5105 and 18F-THK5117. *Alzheimer's & Dementia,*
    10(4), P241.
Villemagne, V. L., Fodero-Tavoletti, M. T., Masters, C. L., & Rowe,
    C. C. (2015). Tau imaging: early progress and future directions.
    The Lancet Neurology, 14(1), 114–124.
Villemagne, V. L., Furumoto, S., Fodero-Tavoletti, M., Harada, R.,
    Mulligan, R. S., Kudo, Y., et al. (2012). The challenges of tau
    imaging. *Future Neurology, 7*(4), 409–421.
Walji, A. M., Hostetler, E. D., Selnick, H., Zeng, Z., Miller, P., Ben-
    nacef, I., et al. (2016). Discovery of 6-(Fluoro-18F)-3-(1H-
    pyrrolo[2,3-c]pyridin- 1-yl)isoquinolin-5-amine ([18F]-MK-
    6240): A Positron Emission Tomography (PET) imaging agent
    for quantification of neurofibrillary tangles (NFTs). *Journal of*
    Medicinal Chemistry, 59(10), 4778–4789.
Wong, D. F., Borroni, E., Kuwabara, H., George, N., Rosenberg,
    P., Lyketsos, C., et al. (2015). First in-human PET study of

3 novel tau radiopharmaceuticals: [11C]RO6924963 [11C]
    RO6931643, and [18F]RO6958948. *Alzheimer's & Dementia,*
    11(7), P850–P851.
Wood, H. (2013). Alzheimer disease: [11C]PBB3— a new PET ligand
    that identifies tau pathology in the brains of patients with AD.
    Nature Reviews Neurology, 9(11), 599–599.
Wooten, D., Guehl, N. J., Verwer, E. E., Shoup, T. M., Yokell, D. L.,
    Zubcevik, N., et al. (2016). Pharmacokinetic evaluation of the tau
    PET radiotracer [18F]T807 ([18F]AV-1451) in human subjects.
    Journal of Nuclear Medicine, 58(3): 484–491.
Xia, C.-F., Areteaga, J., Chen, G., Gangagharmath, U., Gomez, L. F.,
    Kasi, D., et al. (2013). [18F]T807, a novel tau positron emission
    tomography imaging agent for Alzheimer's disease. *Alzheimer's*
    & Dementia, 9(6), 666–676.
Yanai, K., Harada, R., & Okamura, N. (2016). Advances in the devel-
    opment of tau PET radiotracers and their clinical applications.
    International Journal of Neuropsychopharmacology, 19(Suppl
    1), 9.